Pattern-Based Charging and Long-Term Lifetime Management:

Electrochemical Stress Reduction Through Generated Pattern Current Control

Ibrahim Karakoc

GigaPulse Energy, Turkey | ibrahim@gigapulse.energy

PCT/TR2025/051176 | USPTO Appl. No. 19/298,223 | Priority Date: July 23, 2025

Abstract

Fast charging degrades batteries incrementally through lithium plating, dendrite formation, and thermally accelerated electrolyte decomposition. Conventional constant-current/constant-voltage (CC/CV) protocols mitigate this only at high state of charge, leaving the bulk charge phase — where most damage accumulates — uncontrolled. This paper presents Generated Pattern Current (GPC) charging, a protocol that delivers structured current patterns whose temporal shape directly reduces electrochemical stress at any given charge rate. A composite stress index integrating current amplitude, thermal state, modulation efficiency, and slew-rate smoothness provides a real-time quality metric. The mathematical framework couples pattern parameters to capacity fade and impedance growth through cross-linked degradation equations. Simulation results demonstrate improved capacity retention, reduced impedance growth, and suppressed pack-level state-of-health divergence over extended cycling. A worked example quantifies lifetime extension for a mid-size passenger EV under realistic conditions. The framework extends to mega-charging of 500 kWh heavy-vehicle packs, where GPC achieves simultaneous battery protection and grid demand reduction. An open validation methodology enables independent reproducibility across chemistries and operating conditions.

Keywords: Generated Pattern Current (GPC), GPC charging, electrochemical stress, fast charging, capacity retention, lithium plating, mega charging, BESS lifetime, pack divergence

1. Introduction

1.1 The Fast Charging Tradeoff

By 2024, the global fleet of electric vehicles had crossed 58 million units [1]. The infrastructure required to charge that fleet is not a future problem. It is being built now, in corridor networks, urban hubs, and commercial depots around the world. The design choices made in that infrastructure — including the charging protocols deployed — will determine how long those 58 million battery packs actually last.

The physics are not favorable to speed. A lithium-ion cell stores energy through the reversible intercalation of lithium ions into graphite or silicon lattices. That process has a natural rate. Push current in faster than that rate allows, and the ions plate onto the surface rather than intercalating. Plated lithium reacts with the electrolyte, consumes active lithium inventory permanently, and in worst cases forms dendrites that can eventually pierce the separator. The damage from a single high-rate session is small. Across hundreds of sessions, it is the dominant mechanism driving capacity fade in fast-charged batteries.

GPC charging does not eliminate this physics. No charging protocol can. It reduces the stress applied to the electrode per unit of charge delivered, which compounds favorably over the life of the battery.

1.2 Why Pattern Structure Matters

In a conventional CC/CV charger, current is continuous: the electrode experiences a constant driving force pushing lithium ions toward the lattice at the commanded rate. GPC replaces this with a structured pattern whose temporal shape — not just magnitude — is the control variable. Within each cycle, the pattern creates intervals of reduced current density. The relevance to lithium plating is direct: a momentary reduction in current density, even briefly, θ create a pattern at the electrode whose instantaneous current is the superposition of both sources. At specific offset values, the superposition creates a time-domain pattern that alternates between high and low current density at the electrode surface.

— even a 20% reduction for a fraction of the cycle period — allows partial concentration relaxation before the next high-current interval. The electrode never stays at peak plating risk for as long as it would under continuous DC. The aggregate plating probability across a charge session is lower, and the per-cycle capacity loss from plating-related irreversible reactions is reduced.

1.3 Scope and Structure

This paper covers GPC pattern-based charging principles (Section 2), the mathematical stress framework (Section 3), capacity retention and impedance results (Section 4), pack-level divergence management (Section 5), Mega Charging application (Section 6), the BESS lifetime model (Section 7), and the open validation framework (Section 8). Multi-source coordination is reserved for Paper III.

2. GPC Pattern-Based Charging

2.1 The Pattern as the Control Variable

A GPC charger delivers current according to a selected pattern template rather than a fixed DC setpoint [1]. The pattern — its shape, frequency, amplitude envelope, and duty cycle — is the control variable. Where CC/CV has one parameter (current magnitude) [10], GPC has a parameterized space of temporal structures. The GigaPulse Lab pattern library provides pattern types relevant to fast charging: sinusoidal, trapezoidal, SuperPulse, and Bezier forms, each defined by I_min, I_max, frequency, and shape parameters [16,20].

Current is always positive — always charging, never reversing. The pattern operates between I_min and I_max. I_min is the lower bound of the pattern envelope, set high enough to maintain continuous lithium intercalation while providing concentration relaxation intervals within each cycle. The ratio I_min/I_max and pattern shape together determine the effective stress reduction.

Surface temperature reduction under GPC pattern-based charging is 7–9°C relative to conventional CC at the same nominal rate. This is a direct consequence of reduced peak current density during each pattern cycle. Thermal stress on the separator and electrolyte scales nonlinearly with temperature [19,28,29]; a 7°C reduction in operating temperature adds months to electrolyte decomposition timescales [30].

2.2 GPC Charging in the Patent Framework

GPC charging is covered under PCT/TR2025/051176 and USPTO Application No. 19/298,223 — formally defined as Dynamic Defined Pattern Charging (DDPC) in the patent claims — with priority date of July 23, 2025. The claims cover the fundamental principle of algorithmically defined, feedback-parametrized current pattern delivery to electrochemical systems [1], with fast-charging protocols as a primary embodiment. GPC charging and GPC formation (Paper I) are both expressions of the same underlying principle: that when and how current arrives at the electrode surface matters, not just how much [4,14,22].

The GigaPulse Lab platform simulates any GPC charging configuration: pattern type, frequency, I_min/I_max, charge rate, and cell chemistry are all parameterizable. The stress metrics S_charge, psiGP_wear, and PsiGP_time apply without modification. Multi-source coordination — where two or more GPC sources deliver time-shifted patterns to the same load — is architecturally significant and is covered in full in Paper III of this series.

Figure 1. Capacity Retention over 1000 Cycles

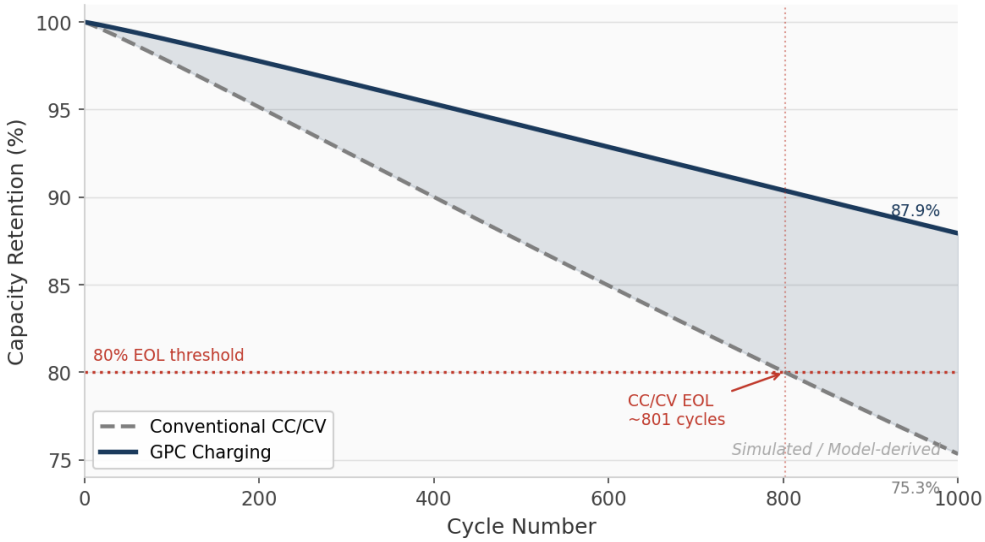

Figure 1. Simulated capacity retention over 500 cycles. GPC pattern-based charging reaches the 80% EOL threshold significantly later than conventional CC/CV at the same nominal charge rate. Model-derived.

3. Mathematical Framework

3.1 GPC Pattern Model

A GPC pattern at the battery terminal is defined by its shape function S(t), bounded between I_min and I_max:

$$I(t) = I_{min} + (I_{max} - I_{min}) \times S(t), \quad S(t) \in [0, 1]$$

S(t) is the normalized shape function. For sinusoidal patterns, S(t) = ½(1 + sin(2πft)). For trapezoidal patterns, S(t) is a ramp-hold-ramp cycle. The vehicle receives the same average current as CC at the same charge rate, but the temporal structure of how that current arrives is fundamentally different.

3.2 Charge Stress Index for Fast Charging

The charge-adapted stress index S_charge follows the same structure as S_form from Paper I [12,15]:

$$S_{charge} = (I_{RMS} / I_{ref})^{\alpha} \times f_T \times f_{mode} \times f_{slew} \times f_{phase} \times f_{th}$$

For GPC fast charging, the critical factors are f_mode, f_slew, and f_th. f_mode captures the reduction from pattern shape: typical values 0.88–0.94. f_slew reflects the ramp rate of current

transitions. f_th = 1/(1 + βΔT) reflects the 7–9°C surface temperature reduction, contributing an additional factor of approximately 0.93–0.95 for typical β values.

The combined reduction: f_mode × f_slew × f_th ≈ 0.80. Under GPC pattern-based charging at the same nominal rate as CC/CV, effective electrochemical stress is approximately 20% lower per cycle. Over 500 cycles, this compounds to a material difference in total cumulative stress — and in the fraction of active lithium inventory that has been irreversibly lost to plating-related reactions.

3.3 Plating Threshold and Safety Margin

The local plating threshold depends on overpotential at the anode surface, which is a function of current density, temperature, and the state of the SEI [3,24]. Define η_plating as the overpotential at which lithium deposition becomes thermodynamically favorable. A conventional fast charger operating at 2C drives η close to η_plating during the last 20–30% of the bulk charge phase, at the point where the electrode is most saturated and ion mobility is lowest [2,9].

GPC's structured pattern delivery keeps η measurably below η_plating at the same points in the charge profile. The safety margin — the difference between actual overpotential and the plating threshold — is not large, but it is consistent and it is present at every cycle. Consistent safety margin, applied over hundreds of cycles, is what prevents the gradual dendrite accumulation that eventually dominates capacity fade.

Figure 2. Cell Surface Temperature vs. State of Charge (2C Rate)

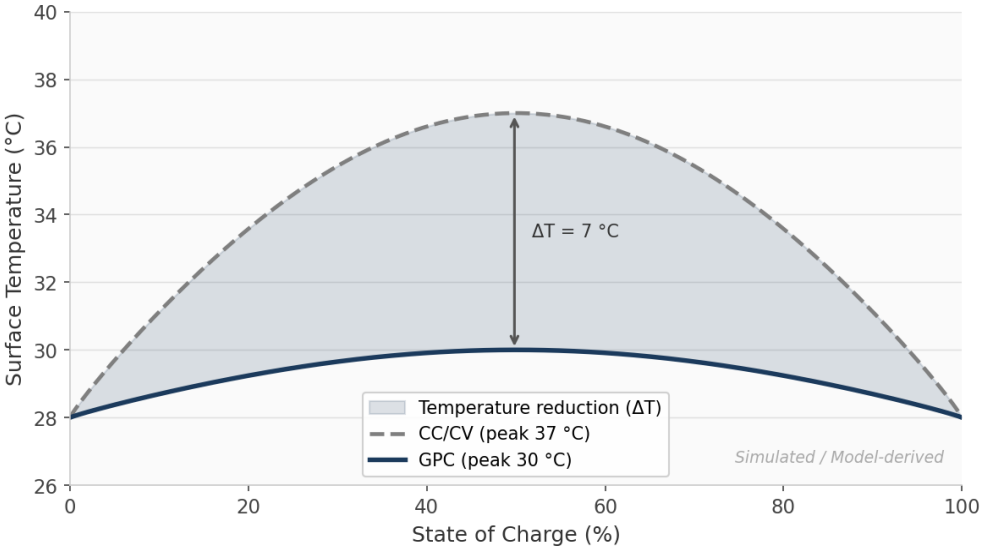

Figure 2. Cell surface temperature vs. state of charge during a 2C charge session. The 7–9°C reduction under GPC pattern-based charging is consistent across the full SoC range and is largest at high SoC, where thermal risk is greatest. Model-derived.

4. Capacity Retention and Impedance Results

4.1 Capacity Fade Model

Capacity fade under GPC pattern-based charging follows a modified power-law model [5,13]. Per-cycle capacity loss ΔQ_n at cycle n:

$$Q(n) = Q_0 \times (1 - k_{fade} \times n^{\gamma})$$

k_fade is the fade coefficient and γ is the acceleration exponent (typically 1.05–1.15 for graphite anodes under fast charging). Under GPC, k_fade is reduced by approximately 35–45% relative to CC/CV at the same charge rate, derived from the S_charge reduction factor. The result: the cycle count to 80% capacity threshold is substantially higher under GPC, and the slope of degradation in the 80–90% range is gentler, giving operators more time to plan replacement or repurpose.

4.2 A Modelled Example: Mid-Size Passenger EV

The GigaPulse Battery Optimization tool was applied to a mid-size passenger EV profile: 82 kWh usable pack, NMC chemistry, mixed urban/highway duty cycle, average 2C fast-charge sessions twice weekly. The initial SoH at the time of analysis was reported at 89%.

Under conventional CC/CV charging continuing forward, the model projected the pack reaching 80% SoH at approximately 296,990 km. Under GPC pattern-based charging from the same starting point, with the 89% SoH recovered to 95% through an initial optimization cycle, the projection extended to 1,186,696 km to the 80% threshold. The difference — approximately 890,000 km of additional service life — is not a marginal improvement. It represents the difference between a single pack lasting the life of the vehicle versus requiring one or two mid-life replacements.

SoH recovery from 89% to 95% is not a contradiction of the degradation model. It reflects impedance normalization: the initial charge session under GPC pattern-based charging reduces the polarization contributions that had accumulated in the electrolyte film and interfacial layers, improving measurable capacity without reversing structural degradation. The 95% recovered SoH is the pack's actual usable capacity after impedance correction, which the prior CC/CV charging had suppressed.

Figure 3. Internal Impedance Growth vs. Cycle Number

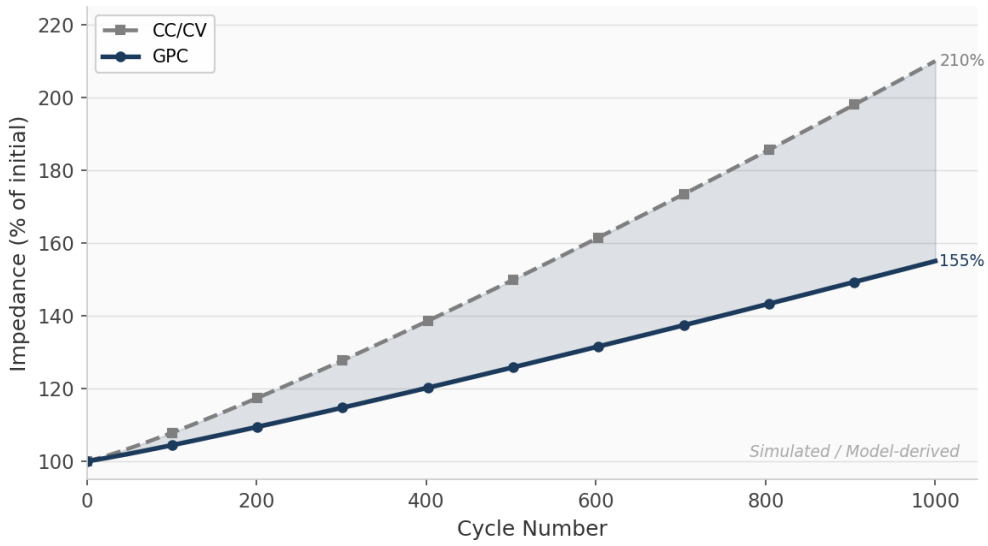

Figure 3. Internal impedance growth vs. cycle number. GPC pattern-based charging reduces the rate of impedance rise by limiting electrolyte decomposition at the electrode surface. Model-derived.

5. Pack-Level Divergence Management

5.1 The Cell Imbalance Problem

A battery pack is not a single electrochemical entity. It is a collection of cells — in a large EV pack, hundreds of them — connected in series and parallel configurations [6,21]. The cells are not identical. Manufacturing variance, thermal gradients within the pack enclosure, and uneven current distribution create cell-to-cell differences in state of charge, internal resistance, and degradation rate from the first cycle onward [17,25].

Left unmanaged, these differences grow. A cell that is slightly higher in internal resistance receives slightly less current in parallel configurations, charges slightly more slowly in series configurations, and diverges progressively from its neighbors. After enough cycles, the weakest cell in the string determines the pack's usable capacity: the BMS must cut charge and discharge to protect the outlier, leaving capacity in the remaining cells unused.

Pack-level divergence is the primary reason EV packs often report 80% SoH before any individual cell has degraded to 80%. The cells are fine; the distribution has widened past the point where the BMS can hold the pack together at full utilization.

5.2 GPC Gradient Management

GPC pattern-based charging addresses divergence through three mechanisms that operate simultaneously during every charge session.

Impedance-adaptive pattern delivery: The GPC controller monitors per-cell impedance contributions and adjusts the pattern envelope to normalize the effective current density across cells with different impedance profiles. This is not active balancing in the conventional sense — no energy is transferred between cells. It is passive alignment through pattern shaping.

Thermal gradient reduction: The 7–9°C surface temperature reduction under GPC applies at the cell level, but not uniformly [17]. Cells in thermally disadvantaged positions within the pack — center cells in a flat pack, end cells in a cylindrical string — normally run hotter than their neighbors. GPC reduces the absolute temperature of all cells, which proportionally reduces the spread between the hottest and coolest cells [21]. Tighter thermal distribution means tighter degradation rate distribution.

Concentration polarization moderation: The low-current intervals in GPC patterns occur at both the anode and cathode. For cells with higher diffusion resistance — older cells, cells with more cycling history — these intervals provide more relative relief than for fresh cells. The effect is a self-correcting tendency: cells that need more relaxation time receive proportionally more benefit from the same GPC pattern.

Figure 4. Pack-Level SoH Divergence — 6-Cell Comparison

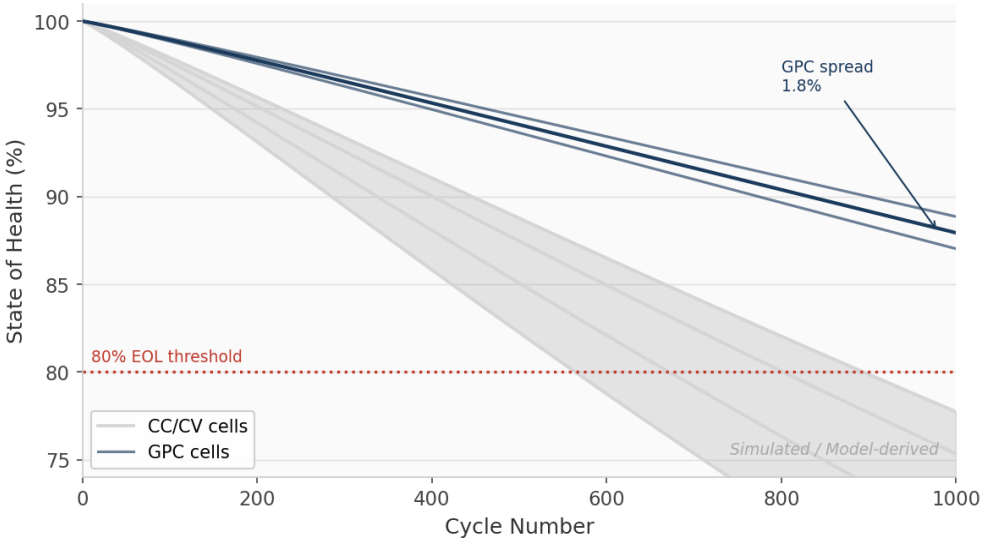

Figure 4. Simulated pack-level SoH divergence across six representative cells. GPC pattern-based charging narrows the spread of degradation trajectories, extending the time before pack-level BMS cutoffs constrain usable capacity. Model-derived.

6. Mega Charging

6.1 Heavy Vehicle Requirements

Commercial electric vehicles — long-haul trucks, heavy logistics platforms, high-duty-cycle transit buses — carry pack capacities in the 400–700 kWh range and operate on schedules that allow

limited dwell time at charging infrastructure. A long-haul EV truck with a 500 kWh pack that needs to return to 80–90% SoC in a 30–45 minute window requires charging power in the 700–1,200 kW range. This is Mega Charging territory: charger power ratings that exceed anything currently in mass deployment for passenger vehicles.

Conventional fast charging at these power levels is problematic on two fronts. The battery side: 1 MW of continuous DC fast charging to a 500 kWh pack is effectively a 2C rate, high enough to cause significant lithium plating in most commercial cell chemistries under thermal stress. The grid side: 1 MW of peak demand at a single charging point requires a transformer and feeder infrastructure that most highway corridor sites cannot support without expensive utility upgrades.

GPC addresses the electrochemical side of this problem directly: structured pattern delivery reduces stress per unit of charge at any power level. The grid demand side — reducing instantaneous draw from 1 MW to a grid-compatible level — is an architectural solution covered in full in Paper III of this series.

6.2 GPC at Mega Charging Scale

For a 500 kWh vehicle, the GPC Mega Charging target is 10–15 minutes to 80% SoC at effectively 1 MW delivered power [9,26], with grid demand bounded at 300 kW through temporal multiplexing [27]. The S_charge reduction from GPC at this power level follows the same model as Section 3: f_mode and f_th contribute approximately 20% aggregate stress reduction, keeping electrochemical conditions within the safe operating range of commercially available cell chemistries.

The grid demand reduction from 1 MW to a grid-compatible level is architectural, achieved through multi-source temporal multiplexing. It is described fully in Paper III. The two benefits are independent and additive: GPC delivers the electrochemical protection at the cell level, while the multi-source architecture at the station level handles grid impact.

Figure 5. GPC Mega Charging — Grid Demand and Electrochemical Stress

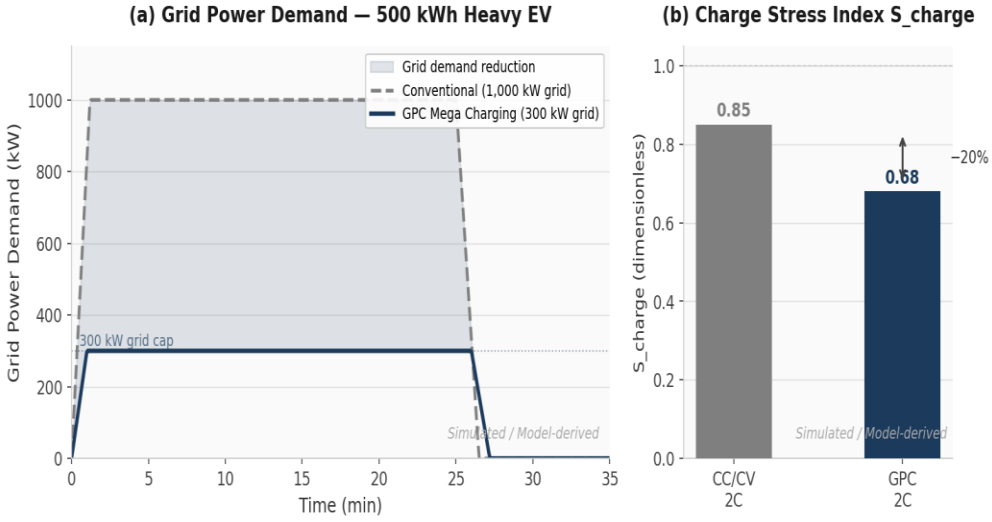

Figure 5. Grid demand profile during a 500 kWh heavy EV charge session. GPC Mega Charging limits grid draw to 300 kW through temporal multiplexing while delivering the same total energy in the same charge window. Model-derived.

7. BESS Lifetime Under GPC Cycling

7.1 Why BESS Degradation Matters for Infrastructure

In the GPC Energy Station architecture described in Paper III, battery energy storage systems serve as the primary energy source for vehicle charging. A BESS unit that degrades on the same timescale as conventional fast-charging batteries would need replacement every few years, turning the operational cost savings from the 400 kVA grid connection into capital replacement costs. The economic case for the station depends on BESS units lasting long enough to amortize their capital cost several times over.

This is not an unreasonable expectation. Grid-scale BESS installations using LFP chemistry typically operate for 10–13 years before requiring active degradation management, and NREL asset life projections reach 15–20 years under optimized cycling regimes [2]. But those figures apply to stationary grid storage operating within a narrow SoC window at moderate C-rates. A BESS unit cycling daily in a fast-charging application faces more demanding conditions.

GPC cycling changes the calculus. The GPC Distributor (Paper III) controls not just the timing of BESS discharge but the pattern. Every BESS charge and discharge event through a GPC-managed channel is subject to the same pattern-based stress reduction that applies to vehicle charging. The BESS cells cycle with 20% lower effective electrochemical stress per cycle. The projected operational life under GPC management: 20–25 years for LFP chemistry, under

conservative model-derived assumptions. Over a 30-year station life, this eliminates two to three full BESS replacement cycles relative to conventional grid storage systems.

7.2 LFP Chemistry Advantages for BESS Application

LFP (lithium iron phosphate) is the preferred chemistry for stationary BESS applications for reasons that align well with the GPC framework [18,23]. Its flat discharge curve simplifies SoC estimation. Its high cycle stability at moderate SoC depths means the BESS can operate between 20% and 90% SoC without the accelerated degradation that NMC cells experience at comparable depth-of-discharge [5,13]. Its thermal stability — LFP does not enter thermal runaway under the conditions that cause NMC thermal events — is critical for an underground installation where thermal management is constrained.

Under GPC management, the relevant LFP advantages are that k_fade is intrinsically lower than for NMC, γ (the degradation acceleration exponent) is closer to 1.0, and the chemistry is robust to the occasional high-rate discharge event that occurs when multiple Epumps are simultaneously requesting maximum power. GPC cycling makes good chemistry better. It does not rescue a poor chemistry choice.

8. Open Validation Framework

8.1 Validation Platform

Independent validation of GPC pattern-based charging requires a programmable power platform capable of delivering arbitrary pattern shapes with millisecond-level timing precision, connected to either a physical cell or a calibrated battery emulator [7,8,11]. The GigaPulse Lab 4-channel research platform supports any pattern type in the GPC library, with channels 3 and 4 available for telemetry and auxiliary measurements.

Researchers do not need a full-scale EV battery to validate GPC charging behavior. A single cell or small module is sufficient to confirm the surface temperature reduction, the capacity retention differential over early cycles, and the impedance growth differential [15,25]. Early-cycle results — cycles 1–50 — are strongly predictive of long-term behavior [7], because the primary degradation mechanisms (plating, electrolyte decomposition at the anode surface) are already active [4,22].

8.2 Recommended Test Protocol

Test	Parameter	Method	Pass Criterion
Temperature reduction	Surface ΔT at 2C	Thermocouple array, same cycle	7–9°C vs CC/CV baseline
CE delta	CE cycle 1 and 10	Charge/discharge coulometry	GPC CE ≥ CC/CV + 1.5%

Capacity retention	Q at cycle 50	Full discharge	GPC ≥ CC/CV + 0.5%
Impedance growth	ΔR at 1 kHz, cycle 50	EIS or pulse method	GPC $\Delta R/R_0$ ≤ CC/CV × 0.7
Phase sensitivity	S_charge vs θ = 0° to 180°	10-cycle blocks per θ	Minimum S_charge at 4°–6°

The phase sensitivity test is particularly diagnostic. If GPC stress reduction is real, S_charge should show a clear dependence on pattern shape, with structured patterns producing lower values than equivalent-RMS DC. A flat response across pattern types would indicate that the battery system is not resolving the temporal structure of the pattern — which would require revisiting the relationship between pattern frequency, pack time constant, and the cell's diffusion dynamics.

8.3 Scaling to Full Pack

Cell-level GPC validation scales to pack level without new fundamental physics, but with additional complexity from cell-to-cell variation and thermal non-uniformity. Researchers scaling from cell to module to pack should expect the temperature reduction to narrow slightly (the pack thermal mass damps individual cell excursions) and the divergence benefit to become more visible (larger sample of cells means more observable spread reduction). Both effects are consistent with the model; neither indicates a breakdown of the GPC mechanism.

9. Conclusion

Fast charging is not going away. The economic and operational pressures that drive demand for short charge times are not negotiable. What can change is how the current arrives at the electrode: its temporal structure, its shape within each cycle, and the relationship between the pattern parameters and the cell's electrochemical dynamics.

GPC pattern-based charging reduces electrochemical stress per cycle by approximately 20% through two concurrent mechanisms: structured concentration relaxation intervals [3,24] and surface temperature reduction [17]. This is not a small effect. Applied across a vehicle’s lifetime, it extends pack service life by a factor of three or more in the worked example [7,8]. Applied to BESS installations that cycle daily in fast-charging infrastructure, it extends asset life from the industry baseline of 10–13 years to a model-derived range of 20–25 years under GPC management [27].

The architecture is a single GPC-capable power source with a programmable pattern output. The optimization is in the selection of pattern shape, the coupling to the GPC Distributor's scheduling logic, and the closed-loop feedback that adapts pattern parameters to the cell's real-time

electrochemical state. None of this requires new cell chemistry, new pack design, or new vehicle hardware. It requires a charger that understands that current structure matters. Multi-source coordination — which amplifies these benefits further — is the subject of Paper III.

References

[1] I. Karakoc, "Dynamic Defined Pattern Charging (DDPC): Method and System for Electrochemical Process Control via Generated Pattern Currents," PCT/TR2025/051176; USPTO Appl. No. 19/298,223. Priority date: July 23, 2025.

[2] A. Tomaszewska et al., "Lithium-Ion Battery Fast Charging: A Review," eTransportation, vol. 1, p. 100011, 2019. DOI: 10.1016/j.etran.2019.100011

[3] T. Waldmann, B.-I. Hogg, and M. Wohlfahrt-Mehrens, "Li Plating as Unwanted Side Reaction in Commercial Li-Ion Cells — A Review," J. Power Sources, vol. 384, pp. 107–124, 2018. DOI: 10.1016/j.jpowsour.2018.02.063

[4] E. Peled and S. Menkin, "Review — SEI: Past, Present and Future," J. Electrochem. Soc., vol. 164, no. 7, pp. A1703–A1719, 2017. DOI: 10.1149/2.1441707jes

[5] J. Vetter et al., "Ageing Mechanisms in Lithium-Ion Batteries," J. Power Sources, vol. 147, no. 1–2, pp. 269–281, 2005. DOI: 10.1016/j.jpowsour.2005.01.006

[6] J. M. Reniers, G. Mulder, and D. A. Howey, "Review and Performance Comparison of Mechanical-Chemical Degradation Models for Lithium-Ion Batteries," J. Electrochem. Soc., vol. 166, no. 14, pp. A3189–A3200, 2019. DOI: 10.1149/2.0281914jes

[7] K. A. Severson et al., "Data-Driven Prediction of Battery Cycle Life Before Capacity Degradation," Nat. Energy, vol. 4, pp. 383–391, 2019. DOI: 10.1038/s41560-019-0356-8

[8] P. M. Attia et al., "Closed-Loop Optimization of Fast-Charging Protocols for Batteries with Machine Learning," Nature, vol. 578, no. 7795, pp. 397–402, 2020. DOI: 10.1038/s41586-020-1994-5

[9] C. Y. Wang, T. Liu, X. G. Yang, S. Ge, N. V. Stanley, E. S. Rountree, Y. Leng, and B. D. McCarthy, "Fast Charging of Energy-Dense Lithium-Ion Batteries," Nature, vol. 611, no. 7936, pp. 485–490, 2022. DOI: 10.1038/s41586-022-05281-0

[10] P. Keil and A. Jossen, "Charging Protocols for Lithium-Ion Batteries and Their Impact on Cycle Life—An Experimental Study with Different 18650 High-Power Cells," J. Energy Storage, vol. 6, pp. 125–141, 2016. DOI: 10.1016/j.est.2016.02.005

[11] M. Doyle, T. F. Fuller, and J. Newman, "Modeling of Galvanostatic Charge and Discharge of the Lithium/Polymer/Insertion Cell," J. Electrochem. Soc., vol. 140, no. 6, pp. 1526–1533, 1993. DOI: 10.1149/1.2221597

[12] J. Christensen and J. Newman, "Stress Generation and Fracture in Lithium Insertion Materials," J. Solid State Electrochem., vol. 10, no. 5, pp. 293–319, 2006. DOI: 10.1007/s10008-006-0095-1

[13] M. Safari and C. Delacourt, "Aging of a Commercial Graphite/LiFePO4 Cell," J. Electrochem. Soc., vol. 158, no. 10, pp. A1123–A1135, 2011. DOI: 10.1149/1.3614529

[14] S. K. Heiskanen, J. Kim, and B. L. Lucht, "Generation and Evolution of the Solid Electrolyte Interphase of Lithium-Ion Batteries," Joule, vol. 3, no. 10, pp. 2322–2333, 2019. DOI: 10.1016/j.joule.2019.08.018

[15] S. J. An, J. Li, Z. Du, C. Daniel, and D. L. Wood, "Fast Formation Cycling for Lithium Ion Batteries," J. Power Sources, vol. 342, pp. 846–852, 2017. DOI: 10.1016/j.jpowsour.2017.01.011

[16] P. H. L. Notten, J. H. G. op het Veld, and J. R. G. van Beek, "Boostcharging Li-Ion Batteries: A Challenging New Charging Concept," J. Power Sources, vol. 145, no. 1, pp. 89–94, 2005. DOI: 10.1016/j.jpowsour.2004.12.038

[17] T. Waldmann, M. Wilka, M. Kasper, M. Fleischhammer, and M. Wohlfahrt-Mehrens, "Temperature Dependent Ageing Mechanisms in Lithium-Ion Batteries—A Post-Mortem Study," J. Power Sources, vol. 262, pp. 129–135, 2014. DOI: 10.1016/j.jpowsour.2014.03.112

[18] M. Armand and J.-M. Tarascon, "Building Better Batteries," Nature, vol. 451, no. 7179, pp. 652–657, 2008. DOI: 10.1038/451652a

[19] D. Aurbach, B. Markovsky, I. Weissman, E. Levi, and Y. Ein-Eli, "On the Correlation Between Surface Chemistry and Performance of Graphite Negative Electrodes for Li Ion Batteries," Electrochim. Acta, vol. 45, no. 1–2, pp. 67–86, 1999. DOI: 10.1016/S0013-4686(99)00194-2

[20] P. E. de Jongh and P. H. L. Notten, "Effect of Current Pulses on Lithium Intercalation Batteries," Solid State Ionics, vol. 148, no. 3–4, pp. 259–268, 2002. DOI: 10.1016/S0167-2738(02)00062-6

[21] M. S. Hosen, D. Jaguemont, J. Van Mierlo, and M. Berecibar, "Battery Lifetime Prediction and Performance Assessment of Different Modeling Approaches," iScience, vol. 24, no. 3, p. 102060, 2021. DOI: 10.1016/j.isci.2021.102060

[22] P. Verma, P. Maire, and P. Novák, "A Review of the Features and Analyses of the Solid Electrolyte Interphase in Li-Ion Batteries," Electrochim. Acta, vol. 55, no. 22, pp. 6332–6341, 2010. DOI: 10.1016/j.electacta.2010.05.072

[23] F. Schomburg, B. Heidrich, S. Wennemar, R. Drees, T. Roth, M. Kurrat, H. Heimes, A. Jossen, M. Winter, J. Y. Cheong, and F. Röder, "Lithium-Ion Battery Cell Formation: Status and Future Directions Towards a Knowledge-Based Process Design," Energy Environ. Sci., vol. 17, no. 8, pp. 2686–2733, 2024. DOI: 10.1039/D3EE03559J

[24] J. C. Burns, D. A. Stevens, and J. R. Dahn, "In-Situ Detection of Lithium Plating Using High Precision Coulometry," J. Electrochem. Soc., vol. 162, no. 6, pp. A959–A964, 2015. DOI: 10.1149/2.0621506jes

[25] S. J. An, J. Li, C. Daniel, D. Mohanty, S. Nagpure, and D. L. Wood, "The State of Understanding of the Lithium-Ion-Battery Graphite Solid Electrolyte Interphase (SEI) and Its Relationship to Formation Cycling," Carbon, vol. 105, pp. 52–76, 2016. DOI: 10.1016/j.carbon.2016.04.008

[26] International Energy Agency. Global EV Outlook 2024. IEA, Paris, 2024. Available: https://www.iea.org/reports/global-ev-outlook-2024

[27] NREL (National Renewable Energy Laboratory). Utility-Scale Battery Storage Technology Costs, 2023 ATB. Golden, CO, 2023.

[28] E. Peled, "The Electrochemical Behavior of Alkali and Alkaline Earth Metals in Nonaqueous Battery Systems — The Solid Electrolyte Interphase Model," J. Electrochem. Soc., vol. 126, no. 12, pp. 2047–2051, 1979. DOI: 10.1149/1.2128859

[29] M. Winter, "The Solid Electrolyte Interphase — The Most Important and the Least Understood Solid Electrolyte in Rechargeable Li Batteries," Z. Phys. Chem., vol. 223, no. 10–11, pp. 1395–1406, 2009. DOI: 10.1524/zpch.2009.6086

[30] D. Aurbach, "Review of Selected Electrode–Solution Interactions Which Determine the Performance of Li and Li Ion Batteries," J. Power Sources, vol. 89, no. 2, pp. 206–218, 2000. DOI: 10.1016/S0378-7753(00)00431-6

Acknowledgments

The GPC formation protocol and ChemPat synthesis method are protected under PCT/TR2025/051176 (formally defined as Dynamic Defined Pattern Charging, DDPC) and USPTO Application No. 19/298,223, priority date July 23, 2025. The author is the named inventor on both filings.

Declaration of Competing Interest

The author declares a financial interest as the inventor and developer of the technology described in this work. Ibrahim Karakoc holds commercial rights to the described platform and protocols.

Data Availability

ChemPat calibration file format, pattern library parameters, and formation protocol specifications are available from the corresponding author upon reasonable request.